Front. Phys. China, 2010, 5(3): 324–329
DOI 10.1007/s11467-010-0109-4

RESEARCH ARTICLE

Sub-diffraction-limited far-field imaging in infrared

Pratik CHATURVEDI, Nicholas X. FANG[†]

Department of Mechanical Science & Engineering, University of Illinois at Urbana-Champaign, 1206 W. Green St., Urbana, IL 61801, USA
E-mail: nicfang@illinois.edu

Received June 1, 2010; accepted June 11, 2010

We investigated a far-field superlens operating at mid-infrared wavelength that allows resolving subwavelength features in the far-field. By utilizing evanescent enhancement provided by surface plasmon excitation of silver nanorods and Moiré effect, we numerically demonstrated that subwavelength information of an object can be converted to propagating information. This information can then be captured by conventional optical components. A simple image reconstruction algorithm can restore the subwavelength object. A sub-diffraction-limited resolution of 2.5 μm at 6-μm wavelength is demonstrated.

Keywords infrared imaging, surface plasmons, subwavelength structures metamaterials, superresolution

PACS numbers 42.79.Bh, 42.70.-a, 42.30.-d

1 Introduction

Infrared (IR) imaging technology such as Fourier transform-infrared (FT-IR) imaging and spectroscopy is one of the most common tools utilized in medicine and the natural sciences for studies of materials and biological species. Measurements conducted in the 1–20 μm region of the electromagnetic spectrum bears special significance, as the absorption of radiation in this region represents signature vibrational, rotational or bending modes of molecules and functional groups. While the FT-IR spectroscopic technique can resolve these narrowband features with high spectral resolution, diffraction-limited spatial resolution is often the bottleneck of this imaging tool. Diffraction-limited performance arises due to the fast decaying nature of subwavelength information contained in the form of evanescent waves. Conventional microscopy is thus capable of capturing only the far-field or propagating components.

In contrast, a planar slab of silver has been demonstrated to achieve subdiffraction resolution in the near-field [1]. This device, termed as superlens, achieves subdiffraction resolution by evanescent enhancement provided by surface plasmon excitation. Silver superlenses operating at near-ultraviolet wavelengths [1, 2], and silicon carbide lenses operating at mid-IR wavelength [3], have demonstrated capability of resolving deep subwavelength features. However, the sub-diffraction-limited resolution capability of these planar superlenses is limited to near-field. This is because, although the evanescent components get enhanced their decaying nature outside the superlens is unaltered and hence, conventional optical components are unable to process this information.

Recently, several different approaches have been proposed to overcome this limitation and obtain subwavelength optical imaging in the far-field [4–6]. The basic idea is to convert the evanescent components with subwavelength information into propagating modes that can be processed by conventional optics. One of the approaches is to utilize the hyperbolic dispersion properties of a strongly anisotropic medium with opposite signs of permittivities ($\varepsilon_{//}$ and $\varepsilon_{\perp}$) [5, 6]. This device termed as hyperlens allows propagation of high-frequency components which ordinarily have an evanescent decay in an isotropic medium. To preserve the propagating nature of these high frequency components even outside the hyperlens, an annular cylindrical geometry is employed. This geometry carries an image magnification, so that the subwavelength features can be magnified to a size that can be seen by conventional diffraction-limited optics. This concept of anisotropic imaging has been experimentally demonstrated to achieve $\sim\lambda/3$ (where λ is the free-space wavelength) resolution at near-ultraviolet wavelengths, utilizing an effective anisotropic medium with concentric rings of metal-dielectric lattice [7, 8]. Extending this technique to the IR regime is difficult because of the choices of materials available to achieve the anisotropy.

An alternative approach is to utilize Moiré effect mediated by excitation of surface plasmons allowing recovery of subwavelength information in the far-field [9]. By carefully designing a subwavelength grating, it is possible to achieve a "frequency mixing" of evanescent fields from the object and grating. In contrast to previous works [4, 9], which utilize a planar superlens to achieve evanescent enhancement and a periodic grating to obtain far-field imaging, in this work, we demonstrate that a discrete array of silver nanorods serves this dual purpose in the IR regime. The nanorods are designed to have plasmonic resonance at mid-IR wavelength and the near-field enhancement associated with this plasmonic resonance fulfills the key requirement for frequency mixing of evanescent fields from the nanorods and the object. This near-field frequency mixing accompanied by the grating momentum of nanorod array leads to the formation of Moiré features that are of propagating nature and can be recorded with a conventional microscope. A simple image reconstruction algorithm can then be utilized to recover subwavelength spatial details of the object from the acquired far-field image (Fig. 1). Our numerical simulations clearly show the formation of Moiré features in the far-field due to evanescent mixing between the nanorods and a periodic object grating. Object features corresponding to 2.5 μm period are recorded in far-field with an incident wavelength of 6 μm, indicating a far-field imaging resolution capability of $\lambda/2.4$. This imaging scheme can be easily interfaced with current FT–IR microscopes and would enable real time imaging with high resolution.

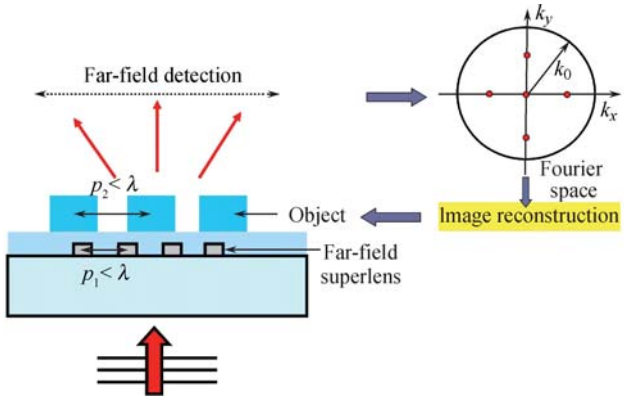

Fig. 1 Sub-diffraction-limited far-field imaging scheme using Moiré effect.

2 Principle of far-field subdiffraction imaging using Moiré effect

The Moiré effect is a well-known optical phenomenon that results in frequency mixing when two periodic/quasiperiodic structures are superposed on each other. The effect is highly sensitive to relative orientation and displacement of the structures and has found unique applications in optical metrology [10]. Historically, like any optical imaging technique, the Moiré effect has also been limited to propagating fields [11]. This is because the evanescent fields from the two structures do not couple to form Moiré fringes. To have evanescent wave mixing, one needs to find a way to enhance the evanescent fields between the two structures. This can be achieved by excitation of surface plasmons which provide the essential enhancement of the evanescent fields. For example, if a near-field silver superlens is inserted in between the two objects, the coupling of evanescent fields can be significantly improved. Thus, frequency mixing of evanescent fields can also lead to formation of Moiré fringes in the far-field [12]. The enhancement and frequency mixing of evanescent fields forms the basis of far-field subwavelength imaging using the Moiré effect. A device so designed has been termed as far-field superlens [4].

The device consists of a periodically corrugated grating. Waves radiated by an object will be diffracted by the grating. The wavevectors of the diffracted waves are given by the grating law $k' = mk^i + nk^g$, where k', k^i, and k^g are the diffracted, incident and grating wavenumbers in the transverse direction, and m, n represent the diffraction order. Since we are interested in resolving subwavelength details of the object, we restrict our discussion to incident wavenumbers that lie in the evanescent region. Out of the diffracted waves, only the ones with $|k'| \leqslant k_0$ are propagating in free-space, where k_0 is free-space wavenumber. This condition can be satisfied if the period of grating and incident field from the object are both subwavelength but with a small difference (e.g. $k' = (k^i - k^g) < k_0$, where $k^i, k^g > k_0$). This results in formation of Moiré fringes in the far-field, provided that the evanescent field from the object couples to the grating. With a proper design of the far-field superlens it is possible to make sure that a unique correlation exists between the far-field Moiré pattern and the near-field subwavelength object [12]. In this case, a simple image restoration algorithm can then be used on the far-field Moiré pattern to reconstruct the object with subwavelength spatial details.

The far-field imaging approach can easily be understood from the frequency domain point of view. Consider a two-dimensional object to be imaged which occupies a double-elliptical area in the spatial frequency domain [Fig. 2(a)]. Conventional lenses are limited to transmitting only the spatial frequencies that lie in the propagation region [Fig. 2(b)]. The image thus obtained does not carry the high-frequency information of the object [Fig. 2(c)]. Let us now imagine a lens specially designed to image only the high-frequency components from the object. The lens suppresses the propagating waves from the object, while enhancing the evanescent waves [Fig. 2(d)]. The lens consists of a periodic grating [Fig. 2(e)].

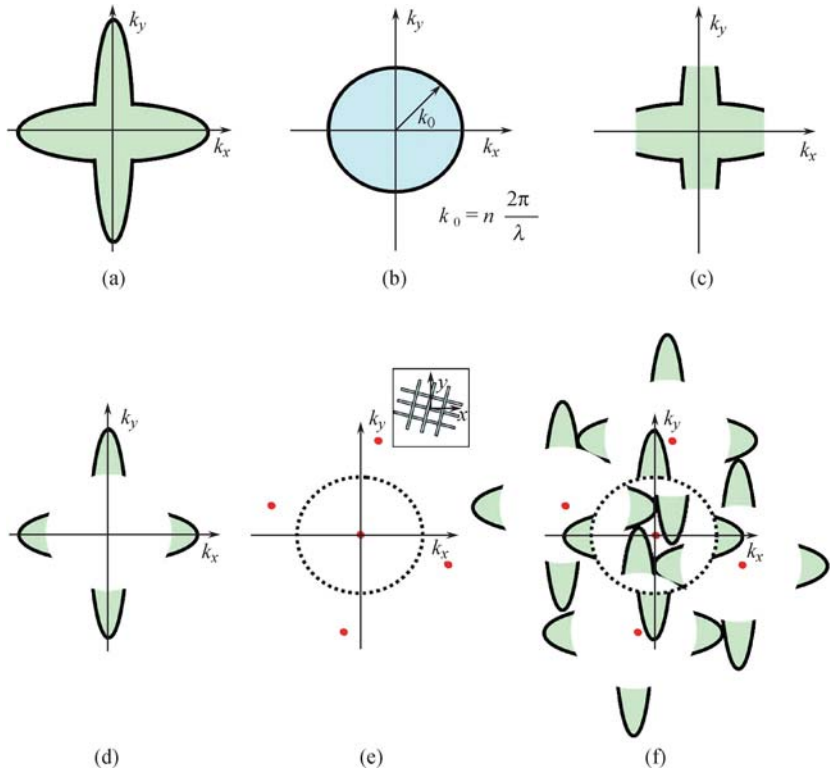

Fig. 2 Frequency domain representation of **(a)** Object, **(b)** Lens, **(c)** Image formed with conventional lens. **(d)** Evanescent components comprising of subwavelength information of the object. **(e)** A rotated two-dimensional periodic grating, dotted circle represents the propagation region. *Inset*: Real space image of grating. **(f)** Image obtained through the grating structure, note that the information lying outside the dotted circle is of decaying nature, and only the information within the dotted circle is carried forward to the far-field.

The evanescent field consisting of subwavelength information of the object couples to this grating. This object field upon diffraction through the grating would result in a pattern which is the convolution of the grating function and the object [Fig. 2(f)]. However, only the features that lie in the propagating region (*marked by dotted circle*) would be carried forward to the far-field. Notice that this far-field transmitted pattern, however, consists of all of the subwavelength information from the object, although in a shifted arrangement. With the knowledge of the grating periodicity of the lens and its orientation, it is possible to reconstruct the image with subwavelength features of the object in the far-field. This forms the basis of subwavelength far-field imaging.

3 Design of far-field superlens in infrared

As mentioned above, a key requirement to achieve Moiré effect for evanescent fields is to ensure field enhancement and coupling between the object and the lens. Surface plasmons provide the essential route to achieve this. However, direct excitation of surface plasmons on a planar interface between metal and dielectric in the infrared regime is limited by the choice of appropriate materials. In order to excite surface plasmons, the metal and dielectric layer should have equal (magnitude) and opposite (sign) permittivities [13]. Moreover, this condition if met for a pair of materials is inherently narrowband because of strong dispersion in permittivities of metals. To address this challenge, we note that the use of discrete plasmonic elements can achieve both goals; first to enhance near-field coupling with the object and second to transform the near-field components to far-field in the form of Moiré features. The use of discrete plasmonic elements also offers the flexibility to tune the operating wavelength by simple variation in geometric parameters.

In this study, we have designed a plasmonic substrate consisting of discrete elements that provide surface plasmon excitation in IR. The substrate consists of a two-dimensional array of Ag nanorods. These nanorods support plasmonic resonance in IR range [14]. The fundamental dipolar resonance of the nanorods (with dimensions 1000 nm × 200 nm × 200 nm) on silicon substrate (mid-IR transparent) is observed at a wavelength of $\lambda =$ 6.1 μm. The nanorod resonance is strongly polarization dependent and is observed only when the electric field is aligned parallel to the rod axis. Figure 3(a) presents the normal incidence far-field transmission spectra of periodic array of nanorods (lattice 2 μm × 2 μm). At resonance, nanorods exhibit strong extinction due to excitation of surface plasmons.

Calculated near-field intensity (∼20 nm above the surface of the nanorods) shows local-field enhancement at

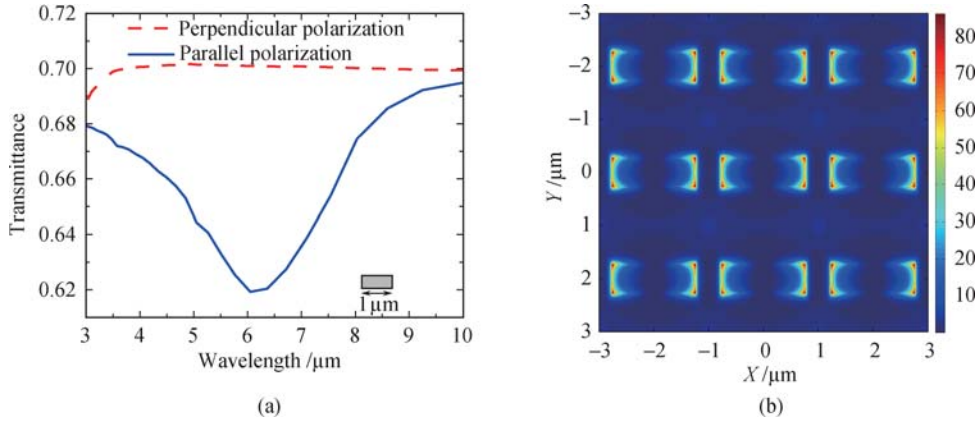

Fig. 3 **(a)** Transmission spectra of periodic array of Ag nanorods in the IR region. Resonance is observed only for parallel polarization, i.e., when the electric field is aligned along the direction of rod axis. **(b)** Near-field intensity calculated 20 nm above the surface of the rods at the fundamental dipolar resonance $\lambda = 6.1$ μm.

the fundamental dipolar resonance [Fig. 3(b)]. In a separate study by Neubrech *et al.* [15], this near-field enhancement has been shown to improve the sensitivity of infrared detection. Utilizing the resonant interaction between surface plasmons and vibrational modes of a molecule, a detection sensitivity of less than one attomole of molecules was demonstrated. In the context of subdiffraction imaging, we show that this near-field enhancement in combination with the grating momentum provided by nanorod array, allows evanescent fields from the object to be diffracted to the far-field. This is evident from Fig. 4, which shows the optical transfer function of nanorod array for evanescent waves calculated at $\lambda =$ 6 μm. The incident evanescent wave is simulated by a total internal reflection mechanism, as illustrated in Fig. 4 inset. It is observed that the far-field transmission of such a nanorod array system is enhanced for wavevectors lying in the region $k^i = 2k_0$ to $4k_0$. Without the nanorod array, evanescent waves have far-field transmission intensity given by $\exp(-2\mathrm{Im}(k_z)z)$, where $k_z = \mathrm{i}\sqrt{k^{i2} - k_0^2}$, which is $< 10^{-9}$ for $k^i > 2k_0$. The enhanced transmission due to nanorods is attributed to surface plasmon excitation, which allows grating coupling of evanescent modes ($2k_0 \leqslant k^i \leqslant 4k_0$) to far-field propagating waves, in accordance with the grating law $k' = k^i - k^g$, where for nanorods $k^g = 3k_0$. In the next section, we numerically demonstrate this coupling effect by computing the far-field spectrum of objects imaged with the nanorod array.

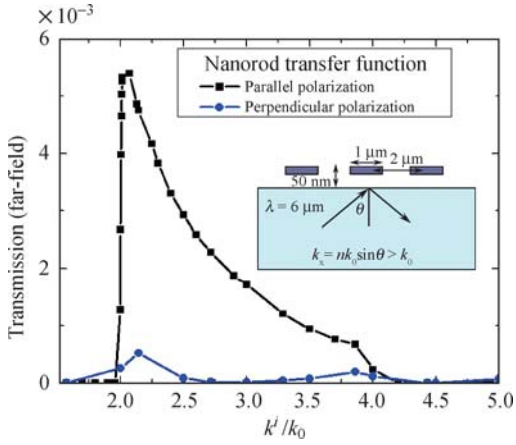

Fig. 4 Far-field transmission computed for various incident transverse wavenumbers at $\lambda = 6$ μm, for parallel and perpendicular polarization. *Inset:* Schematic of the simulation geometry. A total internal reflection mechanism is utilized to simulate evanescent wave incidence on the nanorod array.

4 Computing far-field angular spectrum

To demonstrate far-field imaging numerically, we perform forward computations, i.e., from near-field profile to far-field angular spectrum. As a simplified example, we consider imaging of an aluminum object consisting of a 2-dimensional subwavelength grating. The periodic nature of the object makes the simulation and analysis simpler while capturing the essential physics of the imaging process. The periodicity of the object is chosen to be 2.5 μm × 2.5 μm with linewidth of 1.25 μm. The corresponding lattice constant of plasmonic substrate consisting of array of nanorods is 2 μm × 2 μm. Near the resonance wavelength of the nanorods at $\lambda = 6$ μm, the corresponding wavevectors are $k^i = 2.4k_0$ (object), and $k^g = 3k_0$ (nanorods). It can be seen that diffracted waves corresponding to the evanescent wave mixing of these wavevector components are propagating only through first order diffraction $k' = k^i - k^g = 0.6k_0$. Hence, there is no overlap between diffracted waves and a clear one-to-one relationship exists between far-field angular spectrum and near-field object profile.

To obtain the far-field angular spectrum, we utilize the fact that in the far-field only contribution to a point of observation is from a plane wave originating from the source and propagating along the radial direction to the point of observation. We have performed numerical simulations to compute the far-field angular spectrum of nanorods overlapped with a subwavelength ob-

ject grating. Simulations are performed using a commercial finite-difference time-domain tool [16]. The nanorods on silicon substrate are physically separated from the subwavelength object grating by a thin (50 nm) dielectric spacer layer. A plane wave illumination is assumed from the substrate side and near-field profile is monitored 50 nm away from the subwavelength object on the air side. Periodic boundary conditions are assumed in x–y directions with a period of 10 μm, which is an integral multiple of the period of the rods and the object. The near-field data (E_x, E_y, E_z) recorded in the simulations is decomposed into plane waves using a far-field projection algorithm which gives the far-field angular spectrum of the field on the surface of a sphere (radius = 1 m). The projected far-field spectrum of the combined near-field (object + nanorods) is shown in Fig. 5(a). The polar plot shows variation of electric field intensity $|E|^2$ as a function of θ and ϕ, where θ, ϕ are the polar and azimuth angles of the spherical coordinate system. The far-field intensity $|E|^2$ (θ, ϕ) is directly related to the Fourier components of the field [17], since in the far-field $k_x = k_0 \sin\theta\cos\phi$, $k_y = k_0 \sin\theta \sin\phi$. Apart from zero frequency (DC) components, we observe hot spots in the far-field angular spectrum at the locations marked by white dotted circles. Lowest frequency diffraction spots occur at $(\theta, \phi) = (36.9°, \pm 90°)$ & $(36.9°, \pm 180°)$, while higher order diffraction features are observed at $(\theta, \phi) = (58°, \pm 45°)$ & $(58°, \pm 135°)$. These locations correspond to wavevectors $(k_x, k_y) = (0, \pm 0.6k_0), (\pm 0.6k_0, 0)$ and $(0.6k_0, \pm 0.6k_0)$, $(-0.6k_0, \pm 0.6k_0)$, respectively. In other words, if a lens were to directly convert these Fourier components of the far-field into a real-space image, we would see a 2-dimensional grating with period of 10 μm × 10 μm for 6 μm illumination wavelength. Clearly, this period corresponds to the period of Moiré fringes which result from the evanescent wave mixing between the nanorods and the object grating. To further illustrate this imaging concept, we compute the far-field angular spectrum for a second object which consists of a 2-dimensional grating with period 3.5 μm × 3.5 μm. The Moiré interference fringes in this case correspond to wavevectors $k' = \left(\frac{6}{2}m + n\frac{6}{3.5}\right)k_0$, where 6 μm is the incident wavelength and 2 μm is the periodicity of nanorods. It is clear that the Moiré features are propagating with the lowest diffraction order corresponding

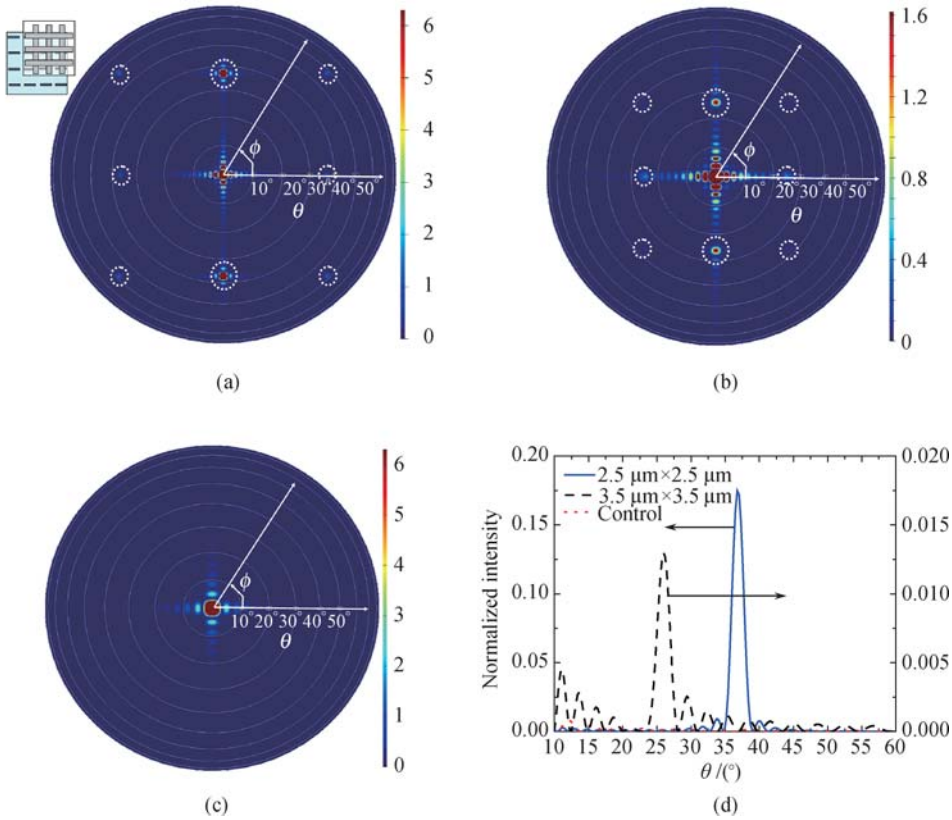

Fig. 5 Computed far-field angular spectrum for a combined system of object and nanorods. In (a) to (c) white solid circles indicate constant θ lines, whereas ϕ varies from 0° to 360° in counterclockwise direction. White dotted circles are marked to highlight the diffraction orders appearing due to Moiré effect. **(a)** Periodic object grating with lattice 2.5 μm × 2.5 μm. *Inset*: Schematic illustration of combined system in real space. **(b)** Object grating with lattice 3.5 μm × 3.5 μm. **(c)** Control case when the incident polarization is perpendicular to the nanorods, resulting in no near-field enhancement. Data presented for object with 2.5 μm × 2.5 μm lattice. **(d)** Far-field angular spectrum for the above three cases at ϕ = 90°. Intensities are normalized to the DC component.

to $m = \pm 1$ and $n = \mp 2$. The corresponding Moiré features have $k' = \mp 0.429 k_0$ which gives $\theta = 25.4°$. These features are indeed recovered in the far-field as illustrated in Fig. 5(b) and (d). As a control case, we also compute the far-field angular spectrum of the combined system (object + nanorods), when the incident wave has a polarization perpendicular to the nanorods. Since, there is no resonance and enhancement of evanescent field in this case, the Moiré features are not observed in the far-field [Fig. 5(c), (d)].

It is evident that the far-field angular spectrum is not the real-space image of the object. However, the real-space image can be reconstructed by applying lateral shifts to the frequency components according to grating law and taking inverse Fourier transform. For the case of periodic grating objects, this procedure is almost trivial. However, the imaging itself is not limited to periodic objects and can be extended to generalized shapes, provided a clear one-to-one relationship is known between the recorded far-field Moiré features and object features.

5 Conclusions

We have numerically demonstrated a far-field imaging technique based on Moiré effect with subdiffraction resolution capability in IR regime. A nanorod substrate was designed that provides near-field enhancement, a necessary precursor to achieve evanescent mixing. By transforming unresolvable high-frequency information of the object into low frequency Moiré features, we are able to observe the subdiffraction features in the far-field. At an incident wavelength of 6 μm, Moiré features corresponding to object periodicity of 2.5 μm were clearly seen in the far-field. The methodology relies on a prerequisite that an unambiguous reconstruction can be done by a suitable design of plasmonic substrate. The image reconstruction procedure is very simple and requires only Fourier transform and lateral shifts of frequency components. This reconstruction procedure can be completely automated, making real time dynamic imaging of materials, biological cells and tissues with subwavelength resolution a distinct possibility.

Acknowledgements The authors are thankful to post doctoral researcher Kin Hung Fung, and Prof. Rohit Bhargava of University of Illinois for several informal discussions. The authors also acknowledge the technical support and assistance received from James Pond and Chris Kopetski of Lumerical Solutions Inc. The authors are grateful for the financial support from the Defense Advanced Research Projects Agency (Grant No. HR0011-05-3-0002), Office of Naval Research (Grant No. N00173-07-G013) and National Science Foundation (Grant No. CMMI-0709023).

References

1. N. Fang, H. Lee, C. Sun, and X. Zhang, Science, 2005, 308: 534
2. P. Chaturvedi, K. Hsu, S. Zhang, and N. Fang, MRS Bull., 2008, 33: 915
3. T. Taubner, D. Korobkin, Y. Urzhumov, G. Shvets, and R. Hillenbrand, Science, 2006, 313: 1595
4. Z. Liu, S. Durant, H. Lee, Y. Pikus, N. Fang, Y. Xiong, C. Sun, and X. Zhang, Nano Lett., 2007, 7: 403
5. Z. Jacob, L. V. Alekseyev, and E. Narimanov, Opt. Express, 2006, 14: 8247
6. S. Alessandro and E. Nader, Phys. Rev. B, 2006, 74: 075103
7. Z. W. Liu, H. Lee, Y. Xiong, C. Sun, and X. Zhang, Science, 2007, 315: 1686
8. I. I. Smolyaninov, Y. J. Hung, and C. C. Davis, Science, 2007, 315: 1699
9. Z. W. Liu, S. Durant, H. Lee, Y. Xiong, Y. Pikus, C. Sun, and X. Zhang, Opt. Lett., 2007, 32: 629
10. D. C. Flanders, H. I. Smith, and S. Austin, Appl. Phys. Lett., 1977, 31: 426
11. M. A. Grimm and A. W. Lohmann, J. Opt. Soc. Am., 1966, 56: 1151
12. S. Durant, Z. W. Liu, J. A. Steele, and X. Zhang, J. Opt. Soc. Am. B, 2006, 23: 2383
13. H. Raether, Surface-Plasmons on Smooth and Rough Surfaces and on Gratings, Springer Tracts in Modern Physics, 1988, Vol. 111: 1–133
14. F. Neubrech, T. Kolb, R. Lovrincic, G. Fahsold, A. Pucci, J. Aizpurua, T. W. Cornelius, M. E. Toimil-Molares, R. Neumann, and S. Karim, Appl. Phys. Lett., 2006, 89: 253104
15. F. Neubrech, A. Pucci, T. W. Cornelius, S. Karim, A. Garcia-Etxarri, and J. Aizpurua, Phys. Rev. Lett., 2008, 101: 157403
16. See http://www.lumerical.com/
17. L. Mandel and E. Wolf, Optical Coherence and Quantum Optics, Cambridge: Cambridge University Press, 1995